Phosphatydylglycerol Promotes Bilayer Insertion of Salmon Calcitonin

Jeremy P. Bradshaw
Department of Preclinical Veterinary Sciences, Royal (Dick) School of Veterinary Sciences, University of Edinburgh, Summerhall, Edinburgh EH9 1QH, Scotland

ABSTRACT Neutron diffraction from oriented multibilayers has been used to study the bilayer interaction of the amphipathic peptide salmon calcitonin. Penetration of calcitonin into bilayers composed of dioleoylphosphatidylcholine increases with the addition of 15% (mol) of the anionic phospholipid dioleoylphosphatidylglycerol. Neutron scattering profiles of water distribution in stacked bilayers show a continuous band of deuterons across each bilayer, consistent with the suggestion that the hormone forms transbilayer α-helixes under these conditions. These experiments add to the growing body of data on the role of phosphatidylglycerol in bilayer insertion of protein helices and suggests a possible evolutionary history for calcitonin.

INTRODUCTION

Calcitonin (Ct) is a 32-amino acid polypeptide hormone, whose principal action, in mammalian species, is inhibition of bone resorption. It has been used in the treatment of Paget's disease and osteoporosis. Ct has a single disulfide bridge, between residues 1 and 7, and a C-terminal proline amide residue. The sequences of both termini are highly conserved, whereas the central region is more variable. In all species, this middle region retains hydrophobic amino acids at every third or fourth position, allowing the chain to fold into a helix in which one face is hydrophobic and the other hydrophilic. Circular dichroism has shown that formation of this amphipathic helix is promoted by certain environments, notably by the presence of phosphatidylglycerol phospholipids (Epand et al., 1983). Attempts have been made to correlate the extent of the helix with the biological activity of the hormone, but neither the hydrophobic moment of the helix (Epand et al., 1986b) nor its optimization in synthetic analogs (Moe and Kaiser, 1985) results in increased activity. The discovery that some salmon calcitonin (sCt) analogs with increased biological activity have reduced helix content (Epand et al., 1986a) has reduced the apparent significance of the amphipathic helix; indeed, some analogs have been shown to retain biological activity without the ability to form an amphipathic helix at all (Epand et al., 1988). This has led to the concept that conformational flexibility and long-range interactions between the amino- and carboxyl-terminal regions affect binding to the receptor and/or conformational properties of the receptor-bound hormone.

The concept of conformational flexibility is supported by NMR studies (Wuthrich, 1976) on human Ct (hCt), in aqueous and dimethyl sulfoxide (DMSO) solutions, which suggest a random coil conformation. Further NMR work on both hCt (Motta et al., 1991) and sCt (Motta et al., 1989) using mixtures of DMSO and water, and on sCt in 90% methanol-water (Meadows et al., 1991), have shown that different conformations of the peptide are favored, depending upon the chemical nature of its environment. A primarily extended conformation with aspects of antiparallel β-sheet was reported for both hCt and sCt in DMSO-water mixtures, whereas in methanol-water mixtures, sCt again adopts an extended conformation, but with a helical segment.

The helical segment of sCt extends from Val 8 (or even Thr 6, according to some authors) to Tyr 22, with Pro 23 breaking the helix. In all of the NMR structures there is *cis-trans* isomerization at Pro 23, with 21–25% in the *cis* form. Other NMR work on sCt has shown that the helix only extends to Lys 18 in the *cis* form (Amodeo et al., 1994). Even without this isomerization at Pro 23, Ct is a very flexible peptide. It is clear that the hormone can adopt different elements of secondary structure under different conditions.

The sequence of sCt is as follows:

Cys^{+}-Ser-Asn-Leu-Ser-Thr-Cys-*Val-Leu-Gly-*Lys^{+}-*Leu-Ser-Gln-*Glu^{-}-*Leu-*$His^{\delta+}$-Lys^{+}-*Leu-Gln-Thr-Tyr*-Pro-Arg^{+}-Thr-Asn-Thr-Gly-Ser-Gly-Thr-Pro-NH_2

Residues 1 and 7 are joined by a disulfide linkage. Groups with a charge at body pH are indicated, and residues of the reported amphipathic helix are italicized (Epand et al., 1983).

This paper reports on the interaction of sCt with phospholipid bilayers of two different compositions. Neutron diffraction from oriented phospholipid multibilayers was used to locate the peptide with respect to the bilayers. The primary aim was to investigate whether sCt adopts a different location in bilayers of a composition that promotes α-helix and bilayers of a composition that does not promote this form. The lipids used were 1,2-dioleoyl-*sn*-glycerophosphocholine (DOPC) with 15% (mol) 1,2-dioleoyl-*sn*-glycero-phosphoglycerol (DOPG) in the bilayers that favored α-helix formation.

Received for publication 16 January 1996 and in final form 14 February 1997.

Address reprint requests to Dr. Jeremy P. Bradshaw, Department of Preclinical Veterinary Sciences, Royal (Dick) School of Veterinary Sciences, University of Edinburgh, Summerhall, Edinburgh EH9 1QH, Scotland. Tel.: 0131-650-6139; Fax: 0131-650-6576; E-mail: j.bradshaw@ed.ac.uk.

0006-3495/97/05/2180/07 $2.00

MATERIALS AND METHODS

Materials

Salmon calcitonin was obtained from Sandoz (Basel, Switzerland). DOPC and DOPG were obtained from Sigma Chemical Company (Poole, Dorset, England) and confirmed to be a single species by thin-layer chromatography.

Neutron diffraction

Neutron diffraction measurements were performed on the D16 instrument at the Institut Laue et Langevin (Grenoble, France). Oriented bilayer stacks of phospholipid and peptide were prepared as follows. Samples comprising a total of approximately 20 mg of lipid and peptide were dissolved in pH-adjusted methanol, and each sample was applied to a quartz microscope slide. The solvent was allowed to evaporate in a stream of nitrogen before the slide was dried in vacuo for several hours. Subsequently, the samples were rehydrated for at least 4 h at 37°C over pure water. Four sets of samples were prepared in this way: pure DOPC, DOPC with 15% (mol) DOPG, DOPC with 5% (mol) sCt, and DOPC with 15% (mol) DOPG and 5% (mol) sCt. Similar samples had already been used in x-ray diffraction experiments (data not shown) before the neutron work to ensure that well-oriented bilayers could be made in the presence of sCt. These measurements provided a highly sensitive confirmation that the samples were homogeneous single-phase systems.

After rehydration each quartz slide, bearing its oriented multibilayer phospholipid sample, was placed in the temperature-controlled cell of the D16 instrument along with water baths containing either ^2H_2O or H_2O, where it was allowed a further period of equilibration of 30 min to 1 h. During this period the equilibration process was monitored by recording the angular position of the third or fourth order of lamellar diffraction, which increased as the multibilayers dehydrated and decreased as they took up water from the atmosphere. Each sample was judged to have achieved equilibrium when there was no further shift in the position of the Bragg peaks, and the calculated lamellar repeat distance was that predicted for the experimental conditions by previous x-ray measurements. Any sample that did not fulfill both of these criteria was discarded.

Data processing

Each recorded diffraction pattern consisted of up to eight well-defined orders. The bilayer repeat distance (D) of each sample was determined using the Bragg equation: $n\lambda = 2D \sin\theta$ (where n is the order of diffraction, λ is the wavelength of neutrons, and θ is the Bragg angle). The instrument offset angle for each sample was calculated at the same time by iterative least-squares regression of this equation over all observed orders of diffraction. Once the diffracted intensities had been corrected for detector response and background and then integrated, using the D16 software, correction factors were applied for the Lorentz factor and absorption by the sample (Worcester and Franks, 1976).

Neutron data are routinely phased by carrying out isotopic substitution of H_2O with ^2H_2O (Worcester and Franks, 1976; Büldt et al., 1979; Franks and Leib, 1979; Jacobs and White, 1989). This method had already been used to phase the neutron data from pure DOPC (Bradshaw et al., 1994) and was used in the present study to phase the other data sets.

The diffraction data were placed on a "relative absolute" scale using the elegant procedure developed by White and his co-workers (Wiener et al., 1991; Wiener and White, 1991; Jacobs and White, 1989), whereby known differences in mean scattering density caused by the introduction of other molecules, or by the selective replacement of hydrogen by deuterium, are used to scale the data sets absolutely with respect to the unit cell contents. By this method the relative scaling of each pair of data sets is adjusted until the area under their difference transform is equal to the difference in their total scattering lengths (per unit cell), and the area under the transform of each set is equal to the total scattering length for the unit cell contents. This approach was used in the present study and basically involved using the size of the sCt and ^2H_2O distributions to scale the different sets of data to each other. The results put the profiles on a "relative absolute" scale in which they are scaled with respect to the unit cell contents, but not on an absolute per volume scale. However, before this scaling can be applied, it is necessary to know how much water (or ^2H_2O) is present in each sample.

Determination of water content

The water content of the stacked multibilayers was determined by replicating the samples and their experimental environment using ^{14}C-labeled DOPC and tritiated water (both isotopes from Amersham International, Amersham, England). Labeled lipid, some of which contained 5% sCt, was spread on microscope coverslips, and the solvent was allowed to evaporate away. They were placed, in batches of two or three, in vacuum desiccators containing phosphorus pentoxide overnight, before being allowed to take up moisture from the atmosphere over tritiated water at 37°C. Subsequently, they were quickly transferred to tubes of scintillant, and the amount of each isotope was determined by scintillation counting.

Estimation of errors

The subtraction of sets of neutron diffraction data to produce difference profiles, as shown in Figs. 1–4, may be performed in real or reciprocal (diffraction) space. When the latter approach is used with a variety of deuterium concentrations, any differences in the result can be used as an

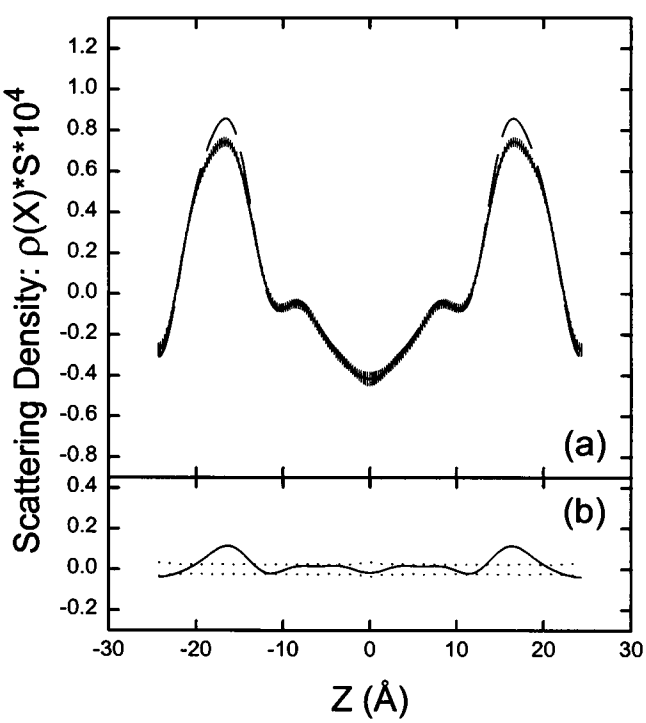

FIGURE 1 (*a*) Neutron scattering density profiles of L_α-phase bilayers of DOPC (Table 1 data set 2, *solid line*) and DOPC with 15% (mol) DOPG (data set 5). The profiles have been calculated by Fourier transformation of the structure factors in Table 1. (*b*) Difference profile calculated by subtracting structure factors for DOPC bilayers from structure factors for DOPC with 15% DOPG bilayers (i.e., data set 5 minus data set 2) and Fourier transforming the result. The main features in this difference profile are the peaks at about ±10 Å caused by neutron scattering from the counterions associated with the phosphate groups of the DOPG. The error bars in *a* and confidence limits in *b* delineate the maximum variation in a large number (1000) of Fourier profiles generated by Monte Carlo sampling of the structure factors and associated errors given in Table 1.

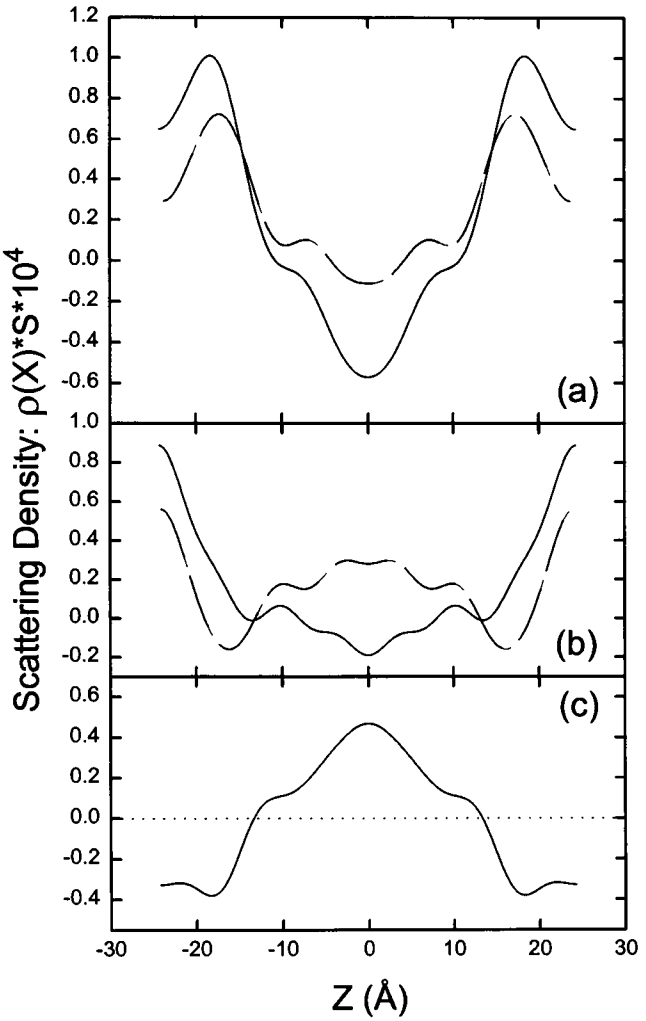

FIGURE 2 (*a*) Neutron scattering density profiles of L_α bilayers of DOPC containing 5% (mol) sCt (Table 1 data set 7, *solid line*) and DOPC bilayers with 15% DOPG and 5% sCt (data set 9, *broken line*). (*b*) Difference profiles showing the effect of subtracting the scattering density due to lipid alone (Fig. 1 *a*) from the profiles shown in *a*, i.e., data sets 7 minus 2 and 9 minus 5. (To reduce the effects of possible termination error caused by a large eighth order in the pure lipid controls and a very small or zero eighth order in the peptide-containing data, the subtraction was carried out over seven orders only.) (*c*) Difference profile calculated by subtracting the solid line in *a* from the broken line, showing the shift in scattering density toward the center of the bilayer upon the introduction of 15% DOPG, i.e., data sets (7 minus 2) minus (9 minus 5).

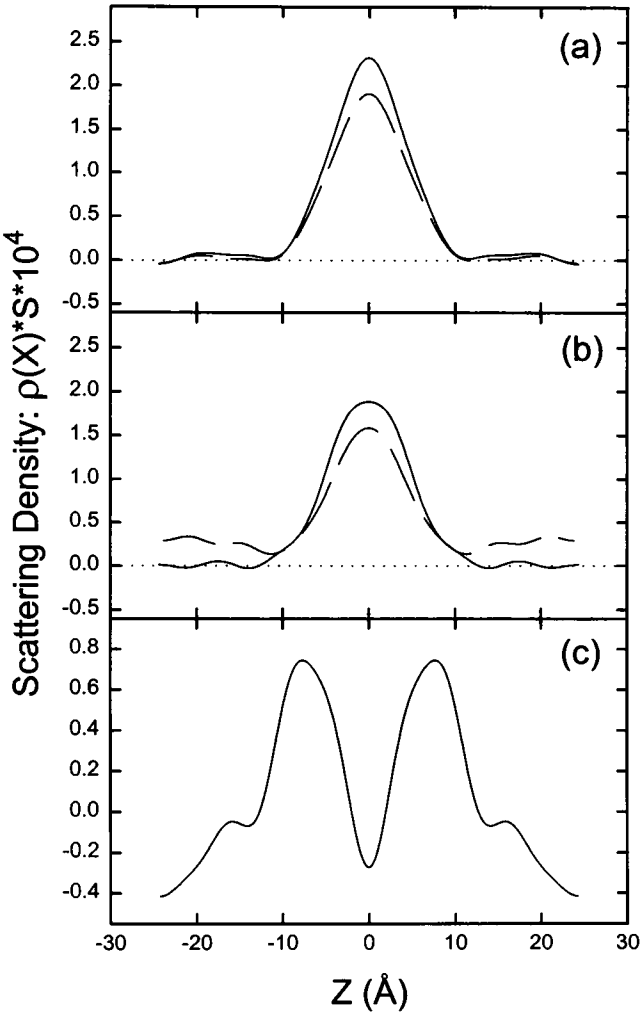

FIGURE 3 The distribution of deuterium, introduced in the form of ^2H_2O, within and between bilayers of (*a*) DOPC (Table 1 data sets 1 minus 2, *solid line*) and DOPC with 15% (mol) DOPG (data sets 4 minus 5, *broken line*). (*b*) DOPC with 5% sCt (data sets 6 minus 7, *solid line*) and DOPC with 15% DOPG and 5% sCt (data sets 8 minus 9, *broken line*). N.B.: For clarity the origin has been switched from the center of the water layer between two adjacent bilayers. Profile *c* is the corresponding profile for pure DOPC bilayers (data set 2), provided for orientation.

estimate of the experimental error in the data points. The errors quoted in Table 1 represent the maximum observed error when this estimation was carried out for each structure factor, over all possible subtractions.

RESULTS AND DISCUSSION

Table 1 contains the experimentally determined, corrected, and scaled structure factors used in the subsequent Fourier transforms and subtractions. The structure factors of pure DOPC have already been published in Bradshaw et al. (1994). The mean lamellar repeat distances (*D*) of the samples were 48.7 ± 0.2 Å, 48.4 ± 0.2 Å, 48.7 ± 0.1 Å, and 48.2 ± 0.6 Å for pure DOPC, DOPC with 15% DOPG, DOPC with 5% sCt, and DOPC with 15% DOPG and 5% sCt, respectively. The corresponding numbers of water molecules per lipid were 5.50 ± 0.10, 5.10 ± 0.30, 5.90 ± 0.15, and 5.30 ± 0.20. The mosaic spread (full width at half-height) of the samples, as determined by the D16 instrument software, varied from 0.4° to 0.6°. These low values are characteristic of unsaturated phospholipids and correlate closely with previous measurements on similar systems (Duff et al., 1993; Bradshaw et al., 1994). The mosaic spread of DOPC bilayers was not significantly affected by the introduction of either DOPG or sCt.

White and co-workers have also reported neutron diffraction data from DOPC. For comparison with the values

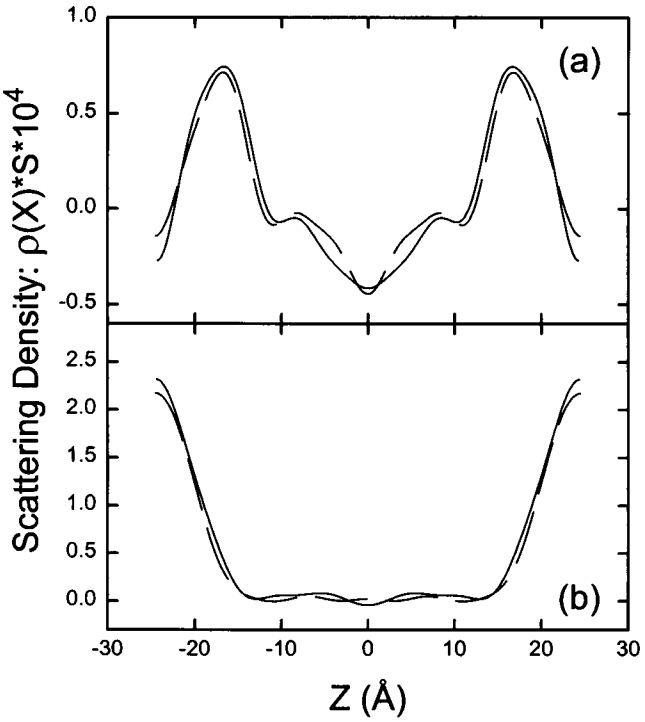

FIGURE 4 A comparison of Fourier transforms calculated from the data given in Table 1 (data set 1, *solid line*) and data published in Wiener et al. (1991) (data set 3, *broken line*). In comparison with the solid line, which represents a DOPC bilayer over pure water at 37°C and 5.5 waters per lipid, the broken line represents a DOPC bilayer at 23°C, 66% relative humidity, and 5.4 waters per lipid. (*a*) Neutron scattering density profiles of L_α-phase bilayers of DOPC. (*b*) The distribution of deuterium, introduced in the form of ^2H_2O, within and between bilayers of DOPC.

reported here, Table 1 includes their published structure factors for stacked DOPC bilayers hydrated with H_2O (from Wiener et al., 1991). The most noticeable differences are in the phase assignment of the fifth order of diffraction and in the value of the seventh order. It is not possible to comment upon whether the phase difference results from the use of different experimental conditions, or whether it is simply caused by an error in phase determination in one of the studies. The differences in the value of the seventh order would seem to support the former suggestion and indicate that the two sets of data refer to different bilayer structures. However, it is notoriously difficult to assign phases to relatively weak orders of diffraction, which contribute relatively little to the bilayer scattering profile. Additionally, the phase determination method most frequently employed, that of $H_2O/^2H_2O$ exchange, is really only effective for the lower orders of diffraction, because such a broad feature as the water distribution function contains little high resolution information. To phase unambiguously the higher orders, it is necessary to supplement the $H_2O/^2H_2O$ with other, more localized additions to the scattering profile. The phase assignments for the structure factors of DOPC have been determined, not just from the experiments reported here, but from a large number of neutron experiments, in some of which extra phase information came from using the difference method with other lipids, including DOPG (as described here) and DOPE (data not shown), and from specific deuteration of the α-, β-, and γ-carbons of the phosphocholine headgroup (data not shown).

Fourier analysis of the diffraction pattern produced when a monochromatic beam of neutrons impinges on the L_α phase of DOPC is shown in Fig. 1. The scattering by the carbons and hydrogens of the alkyl chains in the middle of the membrane is relatively weak, although local maxima are caused by the absence of two hydrogens at the double bond on each chain. Much stronger scattering occurs at the oxygens of the ester linkages and the phosphorus of the headgroup. Also shown is the corresponding profile for DOPC bilayers containing 15% DOPG. The main difference between the two bilayers (*b*) may be attributed to the counterions associating with the anionic DOPG. Each profile was calculated from up to eight orders of diffraction data (Table 1), using established techniques (Bradshaw et al., 1994; Duff et al., 1994).

Fig. 2 *a* shows neutron diffraction profiles for phospholipid bilayers containing 5% sCt. In Fig. 2 *b* are difference profiles, essentially equivalent to the profiles shown in Fig. 2 *a*, but with the scattering due to lipid alone subtracted. Fig. 2 *c* shows the difference calculated by subtracting the solid line of Fig 2 *a* from the broken line. The resulting profile accentuates the difference in neutron scattering density brought about by the addition of DOPG to the DOPC bilayers. There is a clear shift of density away from the aqueous layer into the phospholipid membrane. The interpretation of these difference profiles is complicated by the observation that they do not contain only information about the peptide location in each system, but also changes in phospholipid conformation and water distribution resulting from disruption of the bilayers by the peptide. With a relatively high concentration of peptide (5 molar %), and the relatively low level of hydration (five or six waters per lipid), it is possible that this disruption may be considerable. However, the increase in density within the bilayer and the concomitant reduction of density in the surface and water layers imply increased packing constraints within the hydrophobic region, for which the simplest interpretation is a shift of peptide mass into the bilayer.

Displacements of the functional groups of the phospholipids may be addressed by deuterium labeling of the phospholipids themselves, and will be dealt with in a future paper. The effect of water displacements can be investigated by neutron experiments in which ^2H_2O is introduced into the humid atmosphere within the sample can and thereby taken up into the multibilayer stacks. A difference method may then be used to look at the distribution of water (actually heavy water) in each sample. The results of such subtractions (i.e., sample hydrated with ^2H_2O minus sample hydrated with H_2O) are shown in Fig. 3. The most interesting feature in the water distribution profiles is the continuous band of water spanning the bilayers composed of DOPC with 15% DOPG and 5% sCt. It is not clear from the neutron data alone whether this transbilayer density repre-

TABLE 1 Experimentally determined, corrected, and scaled structure factors used in the Fourier transforms and subtractions

DOPC, 37°C, 100% ^2H_2O							
−28.92 ± 0.24	7.89 ± 0.19	−0.64 ± 0.11	−3.33 ± 0.16	−0.34 ± 0.10	0.84 ± 0.12	0.00	−0.81 ± 0.12
DOPC, 37°C, H_2O							
−8.87 ± 0.19	−5.41 ± 0.17	5.77 ± 0.17	−4.83 ± 0.17	0.50 ± 0.11	0.40 ± 0.10	0.87 ± 0.12	−0.84 ± 0.12
DOPC, H_2O (Wiener et al., 1991)							
−8.00 ± 0.44	−4.51 ± 0.24	4.81 ± 0.25	−5.18 ± 0.29	−0.59 ± 0.08	0.84 ± 0.11	0.00 ± 0.08	−0.94 ± 0.14
DOPC with 15% DOPG, 37°C, 100% ^2H_2O							
−26.22 ± 0.24	5.37 ± 0.17	1.18 ± 0.13	−4.60 ± 0.16	−0.44 ± 0.10	0.95 ± 0.12	0.00	−1.08 ± 0.12
DOPC with 15% DOPG, 37°C, H_2O							
−9.18 ± 0.20	−5.89 ± 0.17	6.65 ± 0.17	−5.65 ± 0.17	0.29 ± 0.09	0.73 ± 0.12	0.76 ± 0.12	−1.02 ± 0.12
DOPC with 5% sCt, 37°C, 100% ^2H_2O							
−35.94 ± 0.26	9.69 ± 0.20	−1.69 ± 0.13	−2.88 ± 0.15	0.25 ± 0.09	0.68 ± 0.11	0.83 ± 0.12	0.00
DOPC with 5% sCt, 37°C, H_2O							
−17.57 ± 0.22	−1.69 ± 0.13	2.47 ± 0.15	−4.02 ± 0.16	−0.35 ± 0.10	0.68 ± 0.11	0.00	0.00
DOPC with 15% DOPG and 5% sCt, 37°C, 100% ^2H_2O							
−18.75 ± 0.22	7.88 ± 0.18	−1.57 ± 0.13	−1.91 ± 0.14	0.24 ± 0.09	0.23 ± 0.09	0.00	0.00
DOPC with 15% DOPG and 5% sCt, 37°C, H_2O							
−8.11 ± 0.19	−1.59 ± 0.12	2.99 ± 0.15	−3.13 ± 0.16	0.00	0.42 ± 0.10	0.24 ± 0.09	0.00

sents free water in some sort of channel, hydration water bound to the surface of the peptide, or simply deuterons that have exchanged with the 60 or so exchangeable protons on the peptide. However, it does show that, in the presence of PG, sCt penetrates very deeply into bilayers of DOPC, possibly even spanning the bilayer from side to side. To adopt such a conformation, the hormone would need to self-associate into multimers, the so-called barrel-stave conformation (Fig. 5 *b*). Comparison of these profiles with corresponding profiles from peptides that are known to adopt a barrel-stave conformation, such as melittin (Bradshaw et al., 1994) and influenza A virus M2 peptide (Duff et al., 1994), shows considerable similarity. All three peptides display the characteristic continuous line of deuterium across the bilayer, although the level of density is considerably reduced in the sCt profile.

The water concentration figures determined by radioisotope labeling are perhaps lower than anticipated when compared to those in the literature, possibly resulting from a temperature gradient within the experimental can. White and co-workers (1987) report a figure of 11 waters per lipid for L_α-phase DOPC at the lower temperature of 23°C. At the higher temperature of 37°C used in the present study, one might expect a similar, or higher, water concentration. However, the low level of errors reported by the double-labeling experiments demonstrates the reproducibility of the measurements, as does the similarly low level of variation in D-spacing observed in the neutron experiments. To confirm the water concentration measurements, the neutron scattering profiles were compared with corresponding profiles calculated from previously published data (Wiener et al., 1991) from L_α-phase DOPC at a similar hydration level. The results are shown in Fig. 4.

The neutron observations reported here suggest that, under the experimental conditions used, sCt is forming multimeric transbilayer structures. There have been no reports of ion channel activity for Ct, but presumably the association of transbilayer α-helices into a barrel-stave arrangement does not necessarily produce an open channel structure. However, there has been a report that Ct stimulates calcium transport in distal convoluted tubule cells, by an unknown mechanism that involves disruption of chloride gradients (Gesek and Friedman, 1993).

Taken together, Figs. 2 and 3 show that the effect upon the bilayer distribution of sCt of introducing DOPG to DOPC bilayers is a shift of peptide deep into the phospholipid layer, possibly even forming transbilayer aggregates of peptide. This correlates well with the observation of increased amounts of α-helix in sCt in the presence of increasing amounts of PG up to 25%, when bilayer solubilization occurs (Epand et al., 1983). Membrane solubilization by amphipathic helices is brought about by the formation of discoidal micelles (see Fig. 5 *c*) at high concentrations of peptide. In these structures the orientation of the helix is also transbilayer, the major difference between the discoidal micelles and the barrel-stave arrangement being the relative proportions of peptide and phospholipid.

Several membrane and membrane-associated proteins are reported to interact with acidic lipids, such as phospholipase C, protein kinase C, myristoylated alanine-rich C kinase, and pp60 (src) (Busher et al., 1995). In the more specific case of PG, a surprising amount of recent literature refers to instances where PG causes rearrangement of secondary structure followed by bilayer insertion, for example, a synthetic 21-amino acid peptide (Gawrisch et al., 1995); the S4 region of *Drosophila Shaker* voltage-gated K^+ channel (Harris et al., 1994; Iwata et al., 1994); a peptide fragment from HIV envelope protein (Gawrisch et al., 1993); and amphiphilic signal sequences from *Escherichia coli* mannitol and glucitol permeases (Portlock et al., 1992). The colicin family of bacterial antibiotic proteins show marked affinity for negatively charged membrane surfaces. A study of the membrane-pore-forming fragment of colicin A (Parker et al., 1989) showed that not only was anionic phospholipid required for membrane association of the protein, but PG was required for induction of the structural

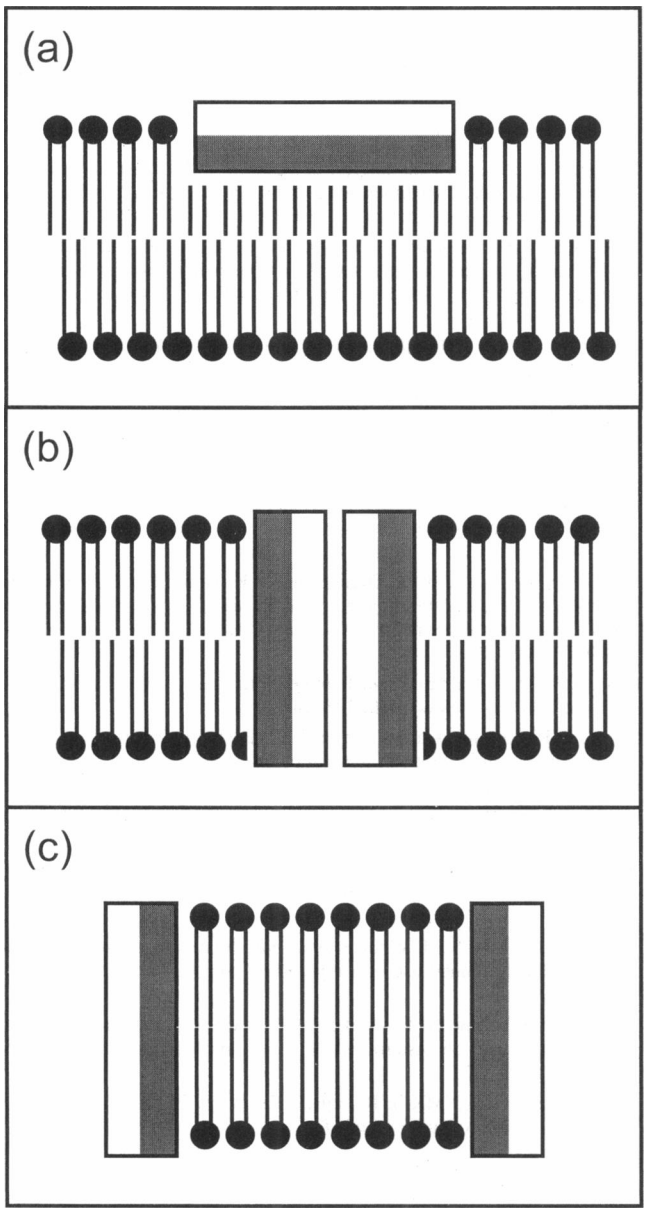

FIGURE 5 Interaction of amphipathic helical peptides with phospholipids. The amphipathic helix is represented as a rectangle with one black (hydrophobic) and one white (hydrophilic) face. In one mode of interaction, surface association (*a*), the helix lies parallel to the bilayer; in the other two, barrel-stave (*a*) and discoidal micelle (*a*), the helix is in transmembrane orientation.

rearrangement whereby insertion of the helical hairpin was achieved. In all of these examples, the nature of the PG-induced structural rearrangement is from random coil to helix, similar to that seen in sCt, although other rearrangements have been reported (e.g., Seelig et al., 1995).

The amphipathic helix of sCt runs from about residues 6–8 to 22–23. Lear et al. (1988) have shown that an idealized amphipathic helix peptide of 14 amino acids fails to form transbilayer complexes because it is too short to span bilayers, whereas a 21-amino acid peptide does. Presumably, if sCt does span bilayers, then nonhelical portions of the peptide must also be involved, a suggestion that is supported by the observation that the membrane-associated helix fails to be induced by PG in partial-sequence peptides representing residues 11–23 of sCt (Epand et al., 1986c). However, longer peptides (residues 1–23) will form helices and produce marked broadening of the gel-liquid crystalline phase transition of DMPG, similar to the effect produced by the intact hormone.

In light of these observations, it is possible to speculate on the mutual arrangement of the positively charged peptide and negatively charged lipid. Much of the positive charge on the peptide is located toward the ends of the molecule. The N-terminus, which is disulfide-bonded to Cys 7, carries a positive charge, as does Lys 11. In a transbilayer orientation of the peptide, it is imagined that these charges would interact with the anionic lipid head groups on one surface of the bilayer. The long side chain of lysine would enable the amino acid itself to penetrate a little deeper into the bilayer, while still maintaining its interaction with the lipid head groups. At the other end of the peptide, Arg 24 would be in a position to complement the negative charge on the opposite surface of the bilayer. This leaves three charged groups unaccounted for, His 17 (with its partial positive charge), Glu 15 (negative), and Lys 18 (positive). It is tempting to speculate that the complementary charges of the latter two could interact in a transbilayer aggregate of an even number of sCT peptides.

Ct is one of the ancient peptide hormones. It has been suggested that it is entirely vestigial in adult humans (Potts, 1976). In light of the neutron results reported here, it is tempting to speculate that the ability to form bundles of transbilayer α-helixes stems from a evolutionary past in which Ct did not interact with a receptor, but brought about its cellular responses by direct ion-channel activity. Such a suggestion would help to explain the conflicting evidence for the importance of α-helix in the functionality of Ct, in terms of completely different evolutionary pressures. The original pressure to develop a transbilayer α-helix multimer would at some point have been overtaken by the drive to optimize peptide-receptor interaction, once the hormone had begun to develop receptor-mediated responses.

The salmon calcitonin was the gift of Sandoz (Basel, Switzerland). Neutron data collection was carried out on instrument D16 at the ILL (Grenoble, France). Gratitude is extended to Dr. Kevin Duff and Dr. Peter Gilchrist for technical assistance.

REFERENCES

Amodeo, P., M. A. C. Morelli, and A. Motta. 1994. Multiple conformations and proline cis-trans isomerization in salmon calcitonin—a combined nuclear-magnetic-resonance, distance geometry and molecular mechanics study. *Biochemistry.* 33:10754–10762.

Bradshaw, J. P., C. E. Dempsey, and A. Watts. 1994. A combined X-ray and neutron diffraction study of selectively deuterated melittin in phospholipid bilayers: effect of pH. *Mol. Membr. Biol.* 11:79–86.

Büldt, G., H. U. Gally, J. Seelig, and G. Zaccai. 1979. Neutron diffraction studies on phosphatidylcholine model membranes. I. Head group conformation. *J. Mol. Biol.* 134:673–691.

Busher, C. A., J. Kim, S. McLaughlin, and R. M. Peitzsch. 1995. Does the binding of clusters of basic residues to acidic lipids induce domain formation in membranes? *Mol. Membr. Biol.* 12:69–75.

Duff, K. C., A. J. Cudmore, and J. P. Bradshaw. 1993. Location of amantadine hydrochloride and free base in dioloeylphosphatidylcholine bilayers by x-ray and neutron diffraction. *Biochim. Biophys. Acta.* 1145: 149–156.

Duff, K. C., P. J. Gilchrist, A. M. Saxena, and J. P. Bradshaw. 1994. Neutron diffraction reveals the site of amantadine blockade in the influenza A M2 channel. *Virology.* 202:287–293.

Epand, R. M., R. F. Epand, and R. C. Orlowski. 1988. Biologically active calcitonin analogues which have minimal interactions with phospholipids. *Biochem. Biophys. Res. Commun.* 152:203–207.

Epand, R. M., R. F. Epand, R. C. Orlowski, R. J. Schlueter, L. T. Boni, and S. W. Hui. 1983. Amphipathic helix and its relationship to the interaction of calcitonin with phospholipids. *Biochemistry.* 22:5074–5084.

Epand, R. M., R. F. Epand, R. C. Orlowski, J. K. Seyler, and R. L. Colescott. 1986a. Conformational flexibility and biological activity of salmon calcitonin. *Biochemistry.* 25:1964–1968.

Epand, R. M., J. K. Seyler, and R. C. Orlowski. 1986b. The hydrophobic moment of the amphipathic helix of salmon calcitonin and biological potency. *Eur. J. Biochem.* 159:125–127.

Epand, R. M., G. L. Stahl, and R. C. Orlowski. 1986c. Conformational and biological properties of partial sequences of salmon calcitonin. *Int. J. Pept. Protein Res.* 27:501–507.

Franks, N. P., and W. R. Leib. 1979. The structure of lipid bilayers and the effects of general anaesthetics: an x-ray and neutron diffraction study. *J. Mol. Biol.* 133:469–500.

Gawrisch, K., J. A. Barry, L. L. Holte, T. Sinnwell, L. D. Bergelson, and J. A. Ferretti. 1995. Role of interactions at the lipid-water interface for domain formation. *Mol. Membr. Biol.* 12:83–88.

Gawrisch, K., K. H. Han, J. S. Yang, L. D. Bergelson, and J. A. Ferretti. 1993. Interaction of the peptide fragment 828–848 of the envelope glycoprotein of human immunodeficiency virus type I with lipid bilayers. *Biochemistry.* 32:3112–3118.

Gesek, F. A., and P. A. Friedman. 1993. Calcitonin stimulates calcium-transport in distal convoluted tubule cells. *Am. J. Physiol.* 264: f744–f751.

Harris, P. I., B. Ramesh, S. Brazier, and D. Chapman. 1994. Role of interactions at the lipid-water interface for domain formation. *FEBS Lett.* 349:371–374.

Iwata, T., S. Lee, O. Oishi, H. Aoyagi, M. Ohno, K. Anzai, Y. Kirino, and G. Sugihara. 1994. Design and synthesis of amphipathic 3(10)-helical peptides and their interactions with phospholipid-bilayers and ion-channel formation. *J. Biol. Chem.* 269:4928–4933.

Jacobs, R. E., and S. H. White. 1989. The nature of the hydrophobic binding of small peptides at the bilayer interface: implications for the insertion of transbilayer helices. *Biochemistry.* 28:3421–3437.

Lear, J. D., Z. R. Wasserman, and W. F. DeGrado. 1988. Synthetic amphiphilic peptide models for protein ion channels. *Science.* 240: 1177–1181.

Meadows, R. P., E. P. Nikonowicz, C. R. Jones, J. W. Bastian, and D. G. Gorenstein. 1991. Two dimensional NMR and structure determination of salmon calcitonin in methanol. *Biochemistry.* 30:1247–1254.

Moe, G. R., and E. T. Kaiser. 1985. Design, synthesis and characterization of a model peptide having potent calcitonin-like biological activity: implications for calcitonin structure activity *Biochemistry.* 24: 1971–1976.

Motta, A., M. A. C. Morelli, N. Goud, and P. A. Temussi. 1989. Sequential, ^{1}H NMR assignment, and secondary structure determination of salmon calcitonin in solution. *Biochemistry.* 28:7996–8002.

Motta, A., P. A. Temussi, E. Wunsch, and G. Bovermann. 1991. A ^{1}H NMR study of human calcitonin in solution. *Biochemistry.* 30: 2364–2371.

Parker, M. W., F. Pattus, A. D. Tucker, and D. Tsernoglou. 1989. Structure of the membrane-pore-forming fragment of colicin A. *Nature.* 337: 93–96.

Portlock, S. H., Y. Lee, J. M. Tomich, and L. K. Tamm 1992. Insertion and folding of the amino-terminal amphiphilic signal sequences of the mannitol and glucitol permeases of *Escherichia coli. J. Biol. Chem.* 267: 11017–11022.

Potts, J. R. 1976. Calcitonin. *In* Peptide Hormones. J. A. Parsons, editor. Macmillan Press, New York. 133–142.

Seelig, J., R. Lehrmann, and E. Terzi. 1995. Domain formation induced by lipid ion and lipid peptide interactions. *Mol. Membr. Biol.* 12:51–57.

White, S. H., R. E. Jacobs, and G. I. King. 1987. Partial specific volumes of lipid and water in mixtures of egg lecithin and water. *Biophys. J.* 52:663–665.

Wiener, M. C., G. I. King, and S. H. White. 1991. Structure of fluid DOPC bilayer determined by joint refinement of X-ray and neutron data. *Biophys. J.* 62:2762–2772.

Wiener, M. C., and S. H. White. 1991. Fluid bilayer structure determination by the combined use of x-ray and neutron diffraction. *Biophys. J.* 59:162–185.

Worcester, D. L., and N. P. Franks. 1976. Structural analysis of hydrated egg lecithin and cholesterol bilayers. II. Neutron diffraction. *J. Mol. Biol.* 100:359–378.

Wuthrich, K. 1976. NMR in Biological Research: Peptides and Proteins. North Holland, Amsterdam. 65–72.